Quasi-isentropic compression by direct laser irradiation of solid samples

Damian C. Swift*and Randall P. Johnson

P-24 Plasma Physics
Los Alamos National Laboratory †
MS E-526
Los Alamos, NM 87545, USA

LA-UR-02-7902 – December 13, 2002; revised January 18, 2004

Abstract

The TRIDENT laser was used to induce dynamic quasi-isentropic compression waves in samples of aluminum, beryllium, and silicon, by irradiating each sample with a pulse whose intensity increased smoothly over ∼2.5 ns. The intensity history of the pulse and the velocity history at the surface of the sample were recorded. Experiments in silicon were performed with samples of two different thicknesses, in which the evolution of the compression wave was clearly visible. An approximate analysis was applied to these data, and compared with theoretical predictions of the isostatic equation of state and of normal stresses produced during uniaxial compression.

*dswift@lanl.gov
†This work was performed under the auspices of the U.S. Department of Energy under contract # W-7405-ENG-36.

Contents

1 Introduction **3**

2 Method **3**
2.1 Samples . . . 3
2.2 Laser drive . . . 4
2.3 Velocimetry . . . 4

3 Results **5**
3.1 Aluminum . . . 5
3.1.1 Shot 14997 . . . 5
3.2 Silicon . . . 5
3.2.1 Shot 14998 . . . 5
3.2.2 Shot 15001 . . . 5
3.2.3 Shot 15005 . . . 7
3.2.4 Shot 15008 . . . 7
3.2.5 Shot 15015 . . . 7
3.2.6 Shot 15018 . . . 7
3.2.7 Shot 15020 . . . 10
3.2.8 Shot 15022 . . . 10

4 Analysis **14**

5 Discussion **17**

6 Conclusions **17**

Change history

18 January 2003 Velocity histories and isentropes corrected for incorrect release window parameter in analysis.

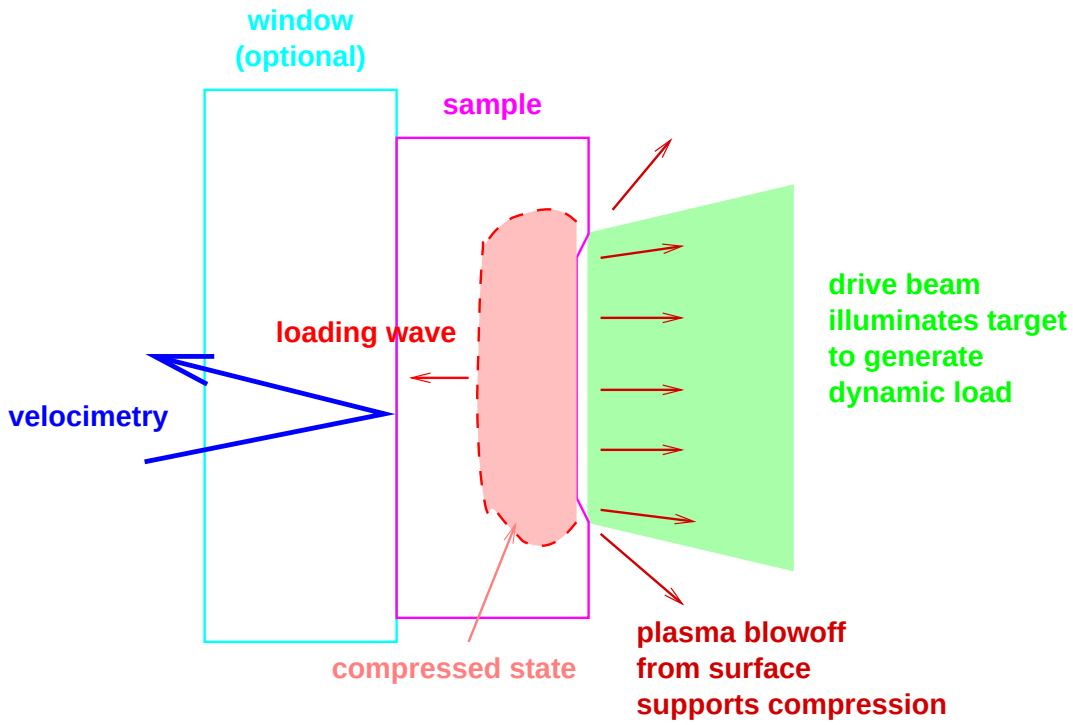

Figure 1: Schematic of direct drive laser loading experiment.

1 Introduction

Dynamic loading along an isentropic path is a valuable complement to shock wave experiments for determining material properties such as the equation of state. Approximately isentropic loading by uniaxial ramp-wave compression has been demonstrated using electrical discharges [1], generally referred to as isentropic compression experiments (ICE). Deviations from an isentropic path are to be expected as a result of uniaxial loading, because any plastic flow that occurs is thermodynamically irreversible.

Laser-induced loading is intended to be broadly isentropic for applications such as inertial confinement fusion. However, laser-induced loading has not to our knowledge been developed or demonstrated for the relatively high precision conditions needed to measure the dynamic response of condensed matter. Here we report the results of experiments performed using temporally shaped laser pulses to induce quasi-isentropic uniaxial loading; the unfortunate but appropriate acronym for this procedure is 'LICE'.

2 Method

A pulse from the TRIDENT laser was directed at one surface of each sample, mounted in the evacuated target chamber. The velocity history of the opposite surface was measured using line-imaging laser Doppler velocimetry (Fig. 1). These experiments were performed during the 'Flying Pig 2' series, during August 2002 [2].

2.1 Samples

The samples used were a few tens of microns thick by several millimeters across. Samples were clamped in a re-usable target holder, which attached magnetically to the TRIDENT target manipulator.

The aluminum and beryllium samples were rolled foils. The silicon samples were (100) crystals, 30 or 59 μm thick. The 30 μm samples were coated with 0.1 μm of aluminum. In all cases, the aluminum coating

faced away from the drive beam, so the drive always irradiated the silicon. A couple of early shots included lithium fluoride windows at the side where velocimetry was obtained.

2.2 Laser drive

The TRIDENT laser is a three beam Nd:glass system with a high degree of flexibility in pulse shaping. TRIDENT was operated in nanosecond mode with frequency doubling to 527 nm (green). The drive pulse comprised 13 elements of 180 ps (full width, half maximum), the intensity of each being controlled through the position of a knife-edge. The relative intensities were chosen to produce an overall envelope which increased smoothly over ∼2.5 ns. The total energy produced in each pulse was measured by diverting a few percent of the energy generated from an uncoated window to a calorimeter. The intensity history was measured similarly, using a photo-diode. The relation between measured and actual energies was calibrated separately for the system as a whole.

As is generally found with high energy and high power lasers, the TRIDENT beams exhibit variations of the order of a factor of two in irradiance over spatial scales of tens of percent of the diameter of the beam. It is highly desirable to have a 1D loading distribution for experiments on dynamic material properties, so a Fresnel zone plate was used to distribute the beam more uniformly on large spatial scales at the expense of variations on spatial scales much smaller than the thickness of the sample. Loading variations caused by the small-scale variations in irradiance are compensated by plasma flow and wave interactions in the first micron or so of the sample, so the bulk of the sample experiences uniform 1D loading. The zone plate used produced a focal spot nominally 4 mm in diameter containing 85% of the nominal energy in the pulse. The plate was imperfect in that the focal spot had a central hotspot; following the usual procedure at TRIDENT the beam was defocused to 5 mm diameter to smear out the hotspot. The resulting drive has never been observed to cause measurable spatial variations in free surface velocity.

In this initial study, we concentrated on experiments sampling pressures up to ∼10 GPa, which were expected to remain isentropic over the sample thicknesses available. The laser energy per pulse was a few tens of Joules.

2.3 Velocimetry

Velocity histories were measured over a line across the sample, on the side opposite to the surface illuminated by the drive pulse. The velocity measurement used a laser Doppler velocimeter of the VISAR type, designed to allow the velocity sensitivity to be altered over a fairly wide range [3]. The VISAR probe laser was a Nd:YAG system operating at 660 nm and producing pulses approximately 50 ns long. The laser beam was spread onto a line on the sample, and the image of the line transferred to the VISAR interferometer. The interference fringes were recorded using a Hamamatsu streak camera.

The delay étalon comprised 4.987" of BK7 glass, giving a velocity sensitivity of 425 km/s/fringe at 660 nm wavelength, taking dispersion and the thickness of the beam-splitters into account.

Temporal fiducials were generated by sending a 200 ps pulse, synchronized to the TRIDENT main oscillator, through a pair of part-silvered mirrors 11.13 ± 0.005" apart. The resulting pulse train, with an interval of 1.886 ± 0.001 ns, was passed through an optical fiber to the slit of the streak camera.

The fringe records were converted to velocity using a procedure developed previously [4]. The locus of each extremum was digitized by constrained optimization, and the velocity history along each extremum was calculated from the displacement from its initial position. Velocity histories at constant positions on the surface were obtained by interpolating from the velocity history along the fringes, using least-squares surface fitting. Both types of velocity history are shown to demonstrate consistency and indicate uncertainties. The uncertainty in the interpolated velocity was less than the scatter in the velocity along different fringes, but gross deviations between the different records indicate regions where the interpolation is less accurate.

Loading histories could be identified as quasi-isentropic if the measured velocity history was continuous, given the temporal resolution of the data. In contrast, shock waves can strictly speaking never be identified without ambiguity from a velocity history (or a radiograph) as it is always possible that the wave is isentropic but smaller than can be resolved experimentally.

Table 1: Laser-induced isentropic compression shots.

Shot	**Target** (μm)	**Energy** (J)	**Comments**
14996	Al (29) / LiF (2000)	9	no drive history; VISAR too weak
14997	Al (29) / LiF (2000)	10	drive history lost; VISAR weak
14998	Si (30)	IR: 9	drive history lost; VISAR weak
15001	Si (30)	11	drive history lost
15005	Si (30)	36	drive spiky; shock structures in velocity
15008	Si (30)	21	
15010	Be (55)	21	VISAR too weak
15013	Al (29)	24	VISAR too weak
15015	Si (30)	27	VISAR weak
15018	Si (30, 59)	33	
15020	Si (30, 59)	62	VISAR weak
15022	Si (30, 59)	13	

3 Results

Unless stated, a ramp drive history and surface velocities were obtained. In a couple of early experiments, no record of drive history was obtained, though measurements of the infra-red intensity within the TRIDENT system gave an idea of whether a smooth ramp was obtained. On some experiments, the drive history was recorded on the oscilloscope, but the digitized record was corrupted; in these cases the shot includes a comment "drive history lost". On one shot the calorimeter recording was too low to be valid; the infra-red energy is quoted instead. On some shots, the VISAR signal was too weak to be used; on others it was weak but usable, in which case the uncertainty in velocity was greater than from a strong signal. In the only experiment on beryllium, the VISAR signal was too weak. These experiments were performed as opportunistic shots in between x-ray diffraction studies. (Table 1.)

3.1 Aluminum

3.1.1 Shot 14997

The only usable VISAR record was from shot 14997, on which the record of the drive history was lost. The drive history itself was observed to be a ramp wave. The sample was 29 μm aluminum foil. A smooth compression and release wave was measured (Fig.2).

3.2 Silicon

3.2.1 Shot 14998

In shot 14998, the laser energy was much less than requested and fell below the sensitivity of the target area calorimeter. The sample was 30 μm (100) silicon, coated with 0.1 μm aluminum on the side observed with the VISAR. A weak compression and release wave was observed, followed later by a reverberation (Fig.3).

3.2.2 Shot 15001

In shot 15001, the drive history was again a smooth ramp, though the record of the pulse shape was lost. The sample was 30 μm (100) silicon, coated with 0.1 μm aluminum on the side observed with the VISAR. Spatial variations were deduced in the velocity though not in the arrival time of features in the velocity history; the variations are probably an artifact of the analysis. A strong compression and release wave was observed, followed by a reduction in fringe contrast and reflected intensity. A reverberation was evident later over part of the spatial region where the reflectivity was adequate. (Fig.4.)

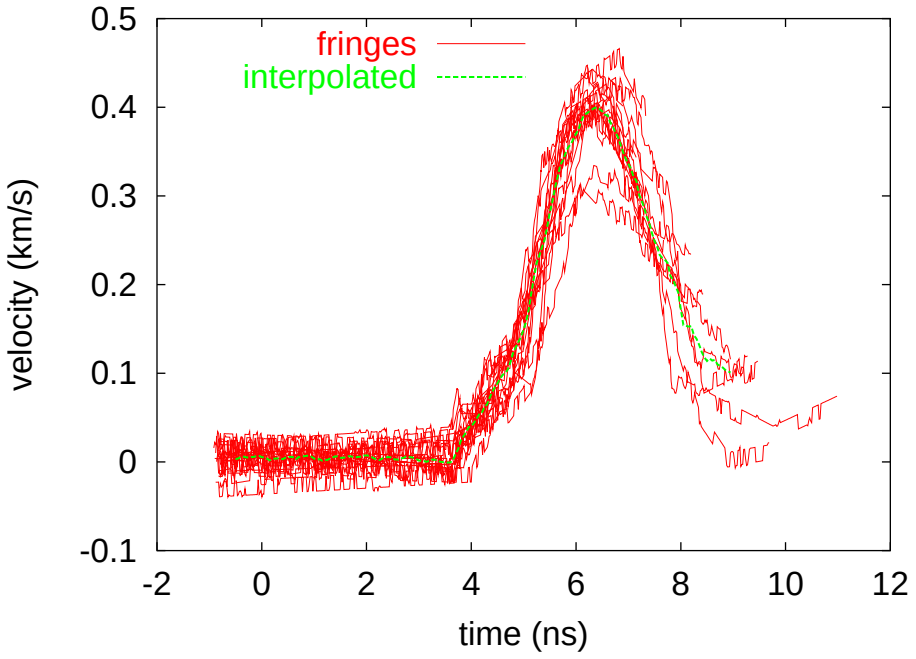

Figure 2: Velocity histories from shot 14997 (29 μm Al / LiF; 10 J).

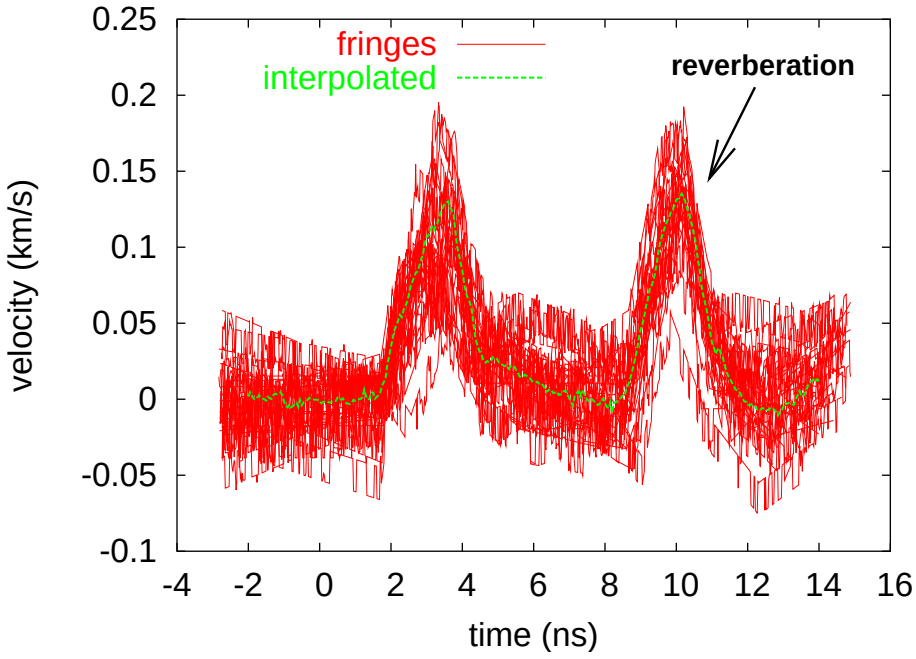

Figure 3: Velocity histories from shot 14998 (30 μm Si; 9 J IR).

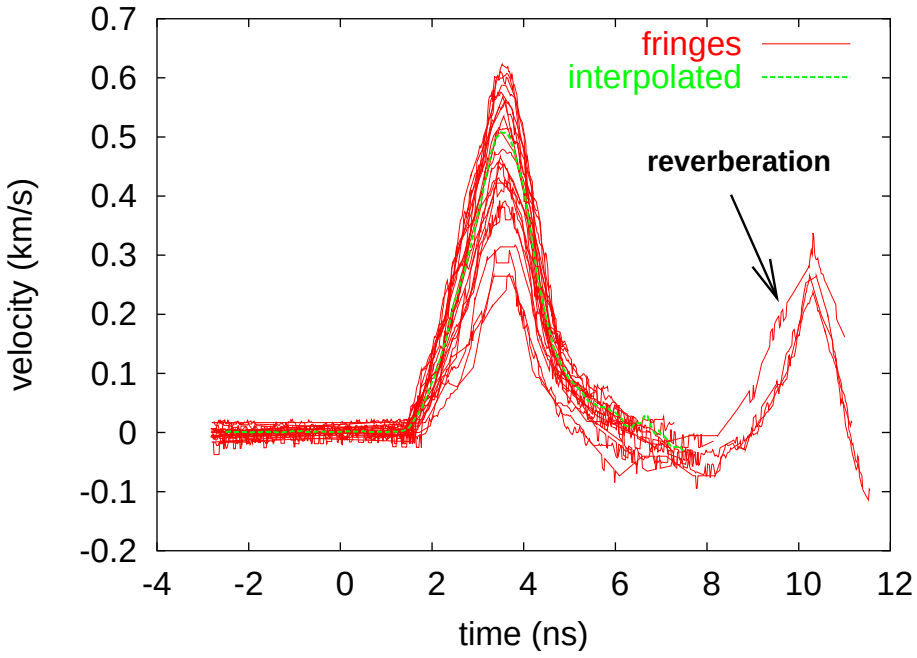

Figure 4: Velocity histories from shot 15001 (30 μm Si; 11 J).

3.2.3 Shot 15005

In shot 15005, the drive history was spiky (Fig. 5) and generated a strong shock in the sample. The reflected intensity and fringe contrast fell rapidly and no useful VISAR data were obtained.

3.2.4 Shot 15008

In shot 15008, the drive history was a smooth ramp (Fig. 6). The sample was 30 μm (100) silicon, coated with 0.1 μm aluminum on the side observed with the VISAR. A smooth compression wave was produced, with a reduction in slope above $\sim$400 m/s. The reflected intensity and fringe contrast fell rapidly in the release part of the wave. (Fig. 7.)

3.2.5 Shot 15015

In shot 15015, the drive history was a fairly smooth ramp (Fig. 8). The sample was 30 μm (100) silicon, coated with 0.1 μm aluminum on the side observed with the VISAR. Spatial variations were deduced in the velocity though not in the arrival time of features in the velocity history; the variations are probably an artifact of the analysis. A strong compression and release wave was observed, followed by a reduction in fringe contrast and reflected intensity. A reverberation was evident later over part of the spatial region where the reflectivity was adequate. (Fig.9.)

3.2.6 Shot 15018

In shot 15018, the drive history was a smooth ramp (Fig. 10). The target consisted of two samples of (100) silicon side-by-side, 30 and 59 μm thick. The thinner sample was coated with 0.1 μm aluminum on the side observed with the VISAR. There was a slight gap between the two samples, and the line VISAR record was affected by shine-through from the drive beam. This distorted and obscured the fringe pattern for a period before velocity-induced fringe motion occurred; this effect did not influence the accuracy of the velocity data. Spatial variations were deduced in the velocity at the surface of the thinner sample though not in the arrival time of features in the velocity history; the variations are probably an artifact of the analysis. A strong

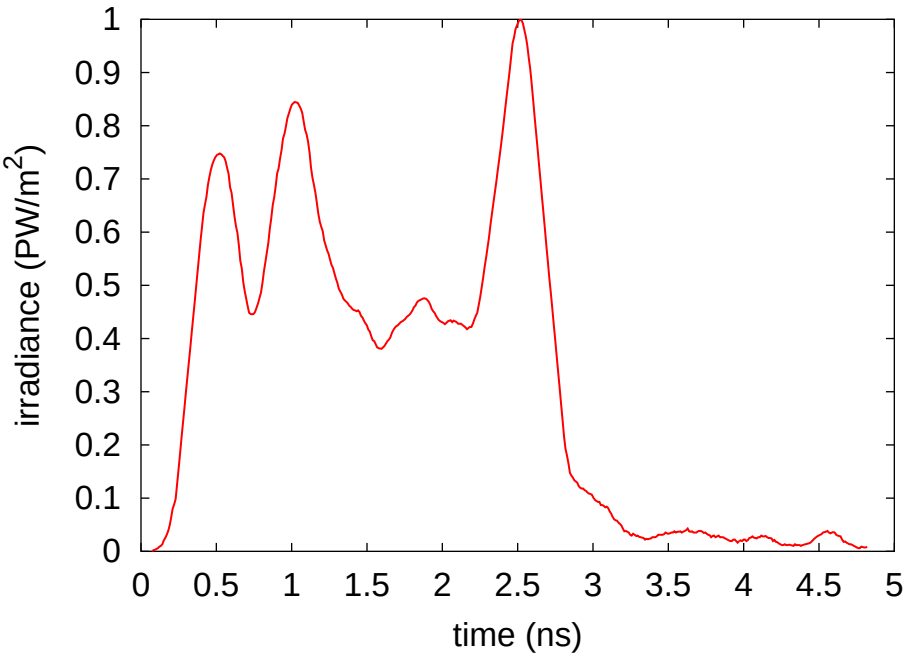

Figure 5: Laser irradiance history from shot 15005 – an inadequate pulse for isentropic compression.

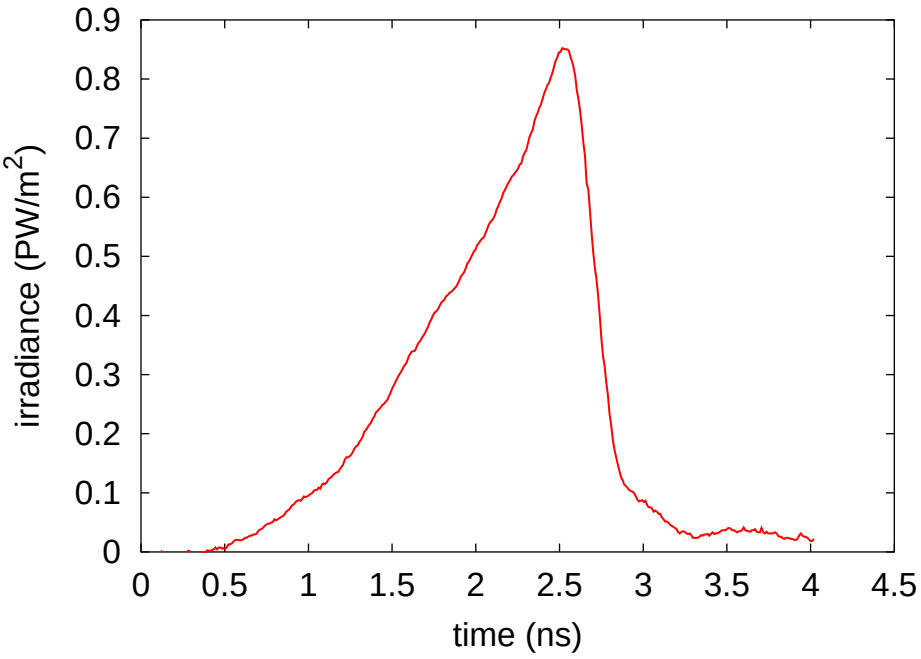

Figure 6: Laser irradiance history from shot 15008.

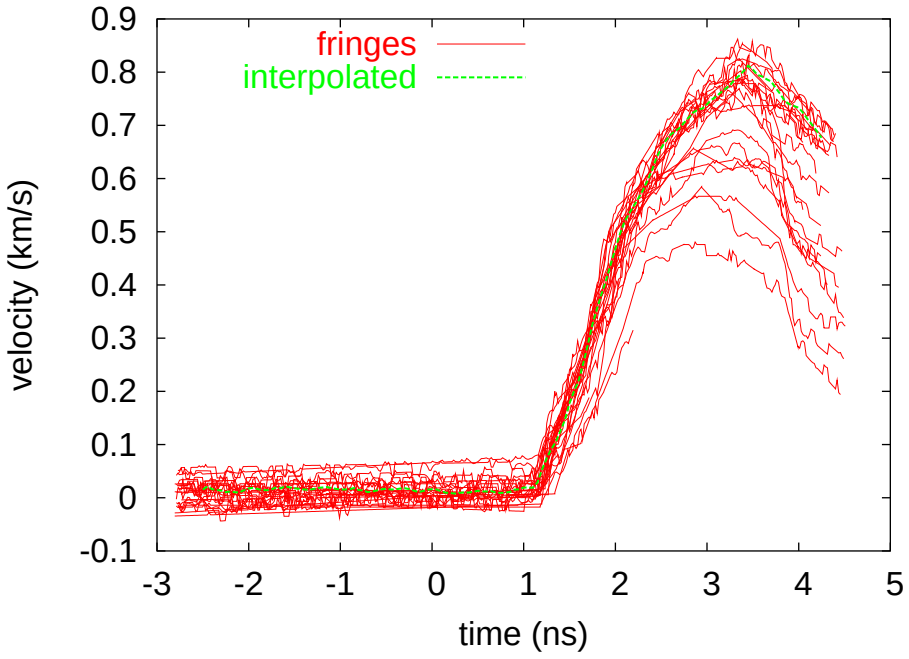

Figure 7: Velocity histories from shot 15008 (30 μm Si; 21 J).

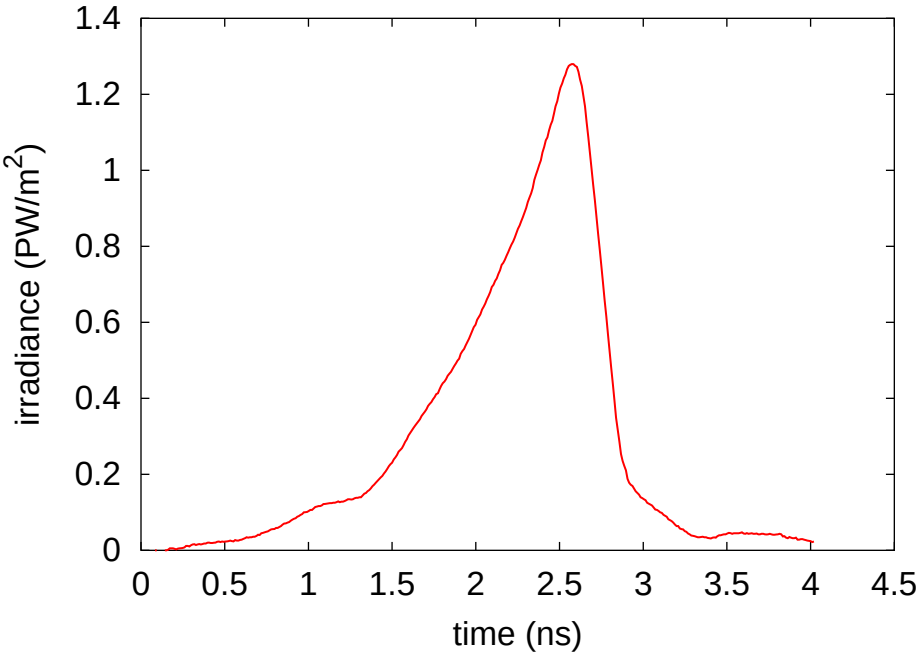

Figure 8: Laser irradiance history from shot 15015.

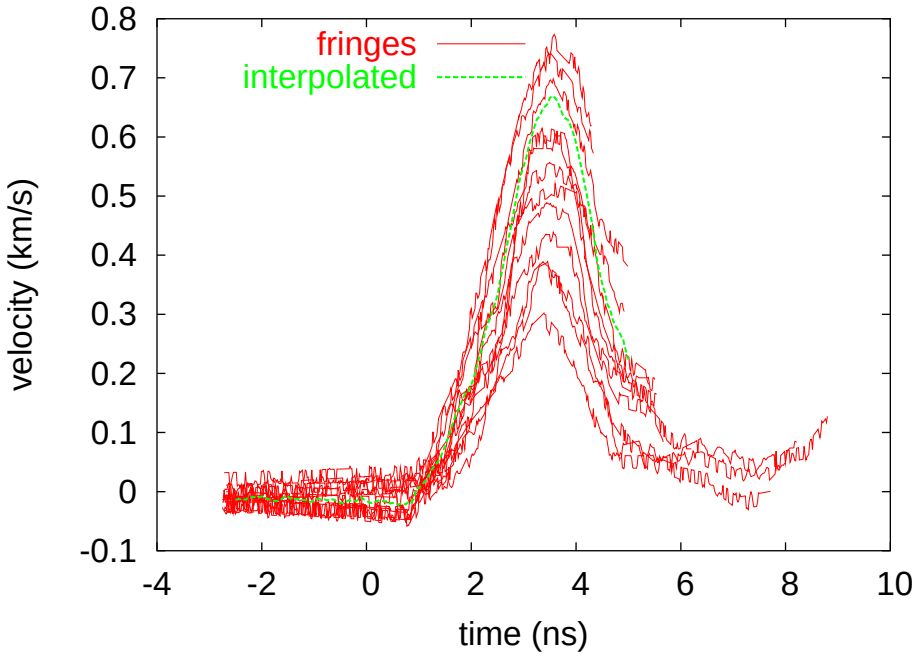

Figure 9: Velocity histories from shot 15015 (30 μm Si; 27 J).

compression and release wave was observed, followed by a reduction in fringe contrast and reflected intensity from the thinner sample. The fringe contrast and intensity from the thicker sample were roughly constant for the duration of the record. (Figs 11 and 12.)

3.2.7 Shot 15020

In shot 15020, the drive history was a smooth ramp (Fig. 13). The target consisted of two samples of (100) silicon side-by-side, 30 and 59 μm thick. The thinner sample was coated with 0.1 μm aluminum on the side observed with the VISAR. A strong compression and release wave was observed, followed by a reduction in fringe contrast and reflected intensity from the thinner sample. The fringe contrast and intensity from the thicker sample were roughly constant for the duration of the record. (Fig.14.)

3.2.8 Shot 15022

In shot 15022, the drive history was a smooth ramp (Fig. 15). The target consisted of two samples of (100) silicon side-by-side, 30 and 59 μm thick. The thinner sample was coated with 0.1 μm aluminum on the side observed with the VISAR. There was a slight gap between the two samples, and the line VISAR record was affected by shine-through from the drive beam. This distorted and obscured the fringe pattern for a period before velocity-induced fringe motion occurred; this effect did not influence the accuracy of the velocity data. Spatial variations were deduced in the velocity at the surface of the thinner sample though not in the arrival time of features in the velocity history; the variations are probably an artifact of the analysis. A strong compression and release wave was observed, followed by a reduction in fringe contrast and reflected intensity from the thinner sample. The fringe contrast and intensity from the thicker sample were roughly constant for the duration of the record. Both samples exhibited a reverberation after the initial compression and release; this was visible over only part of the thinner sample because of the loss of signal. (Fig.16.)

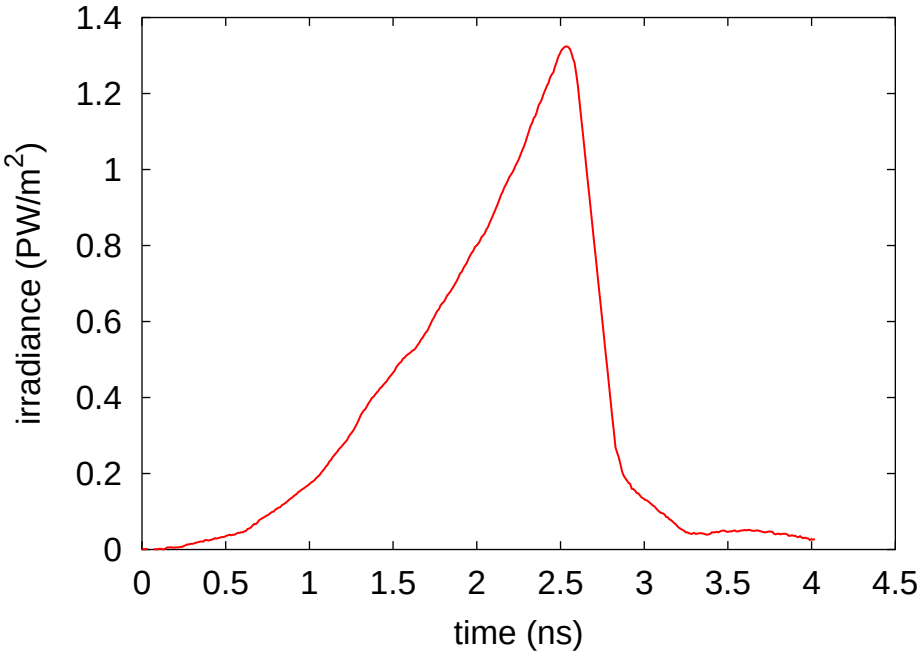

Figure 10: Laser irradiance history from shot 15018.

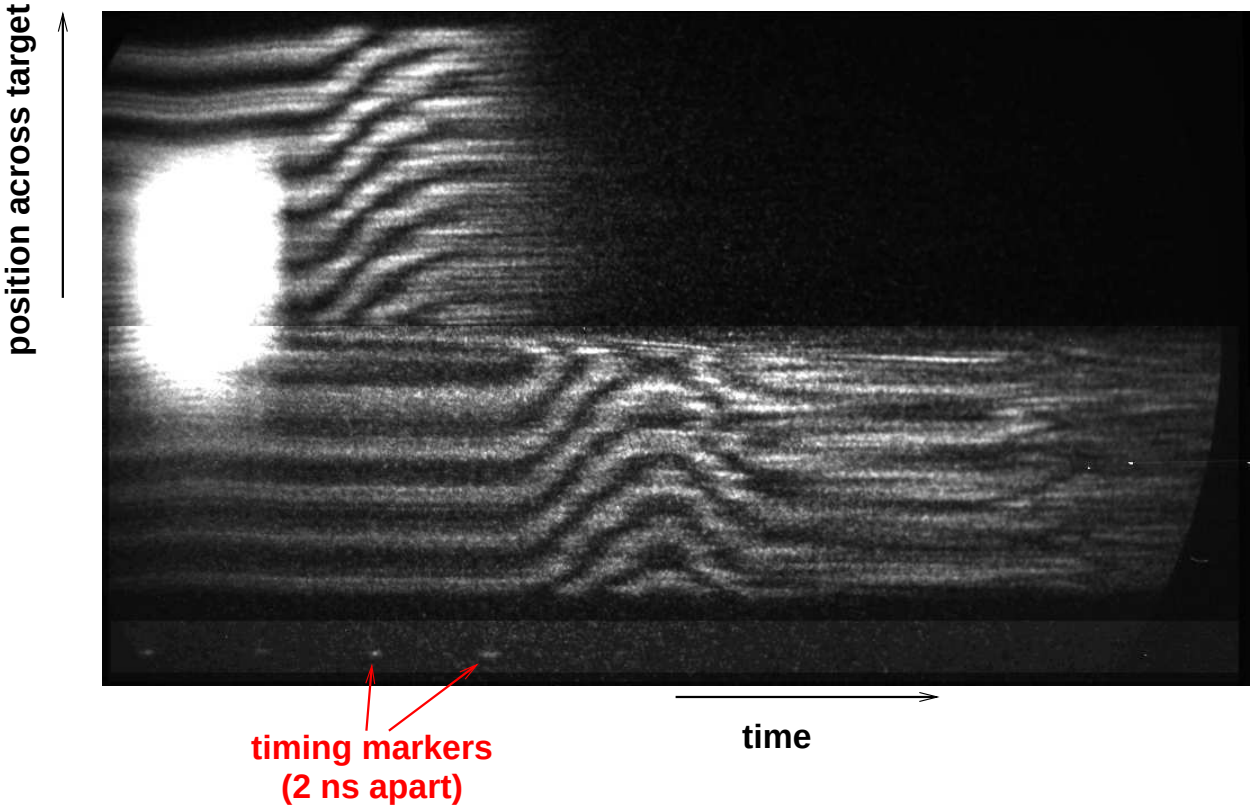

Figure 11: Line VISAR record from shot 15018 (30 and 59 μm Si; 33 J).

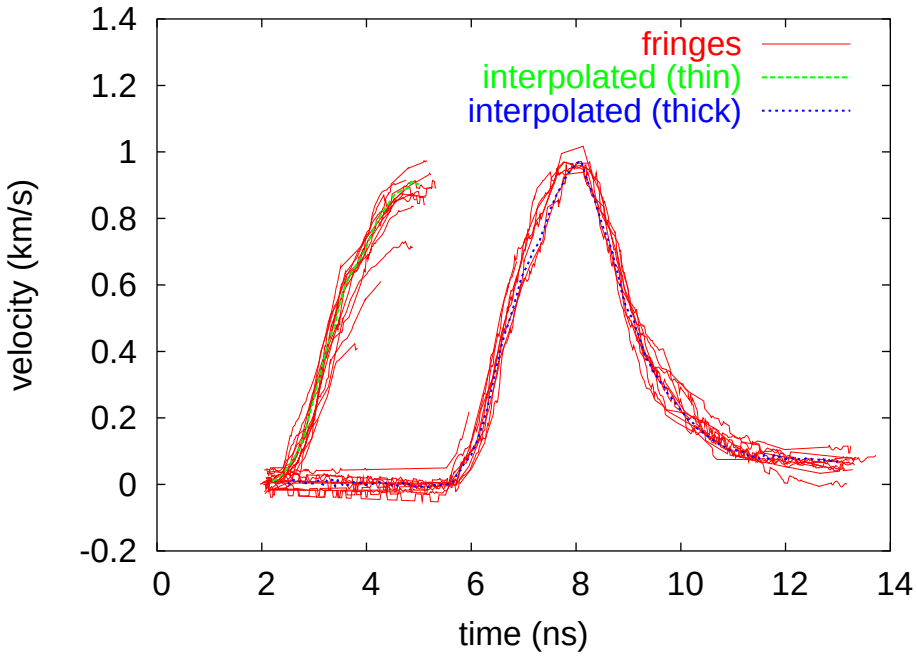

Figure 12: Velocity histories from shot 15018 (30 and 59 μm Si; 33 J).

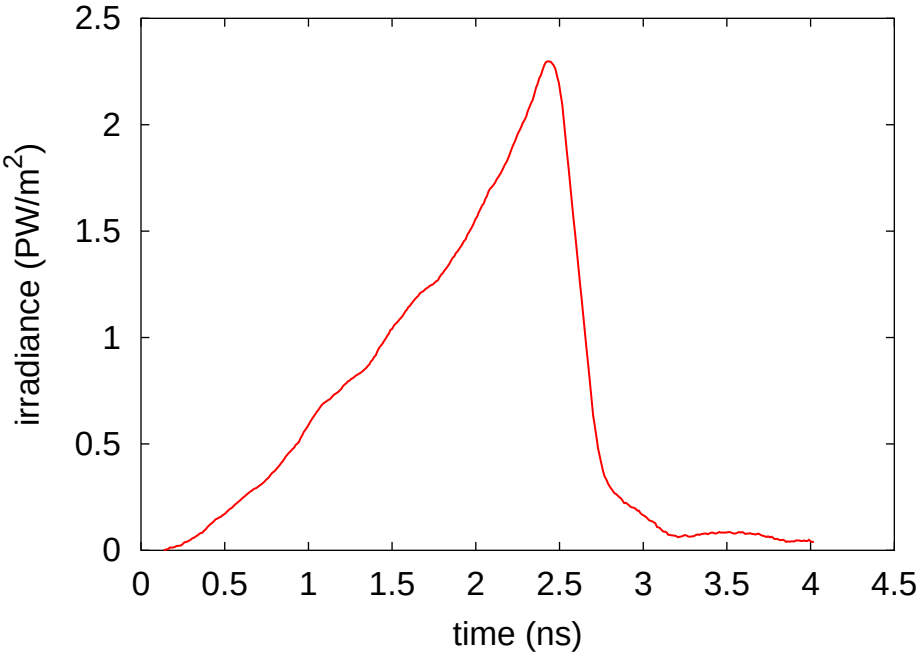

Figure 13: Laser irradiance history from shot 15020.

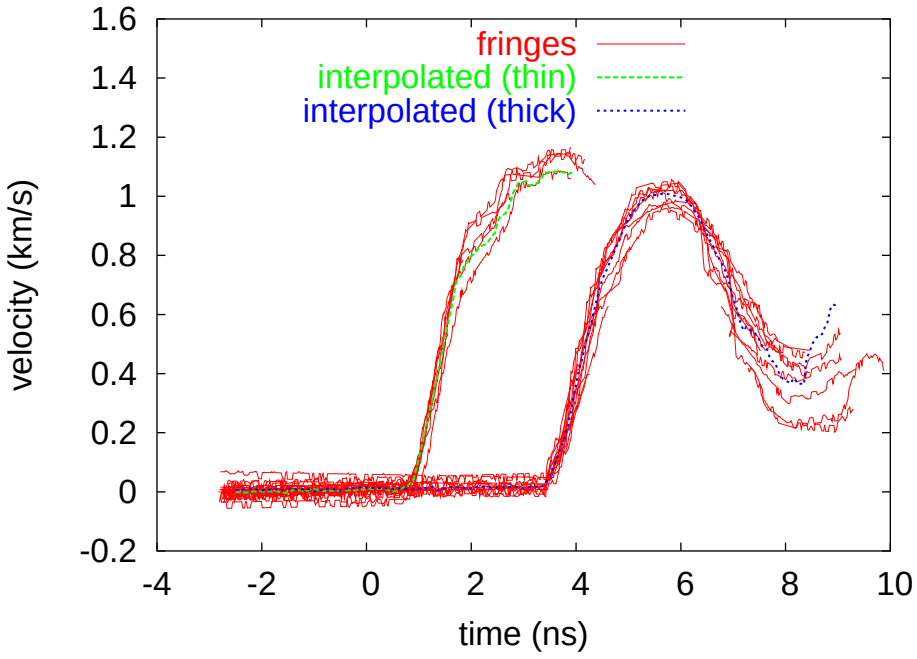

Figure 14: Velocity histories from shot 15020 (30 and 59 μm Si; 62 J).

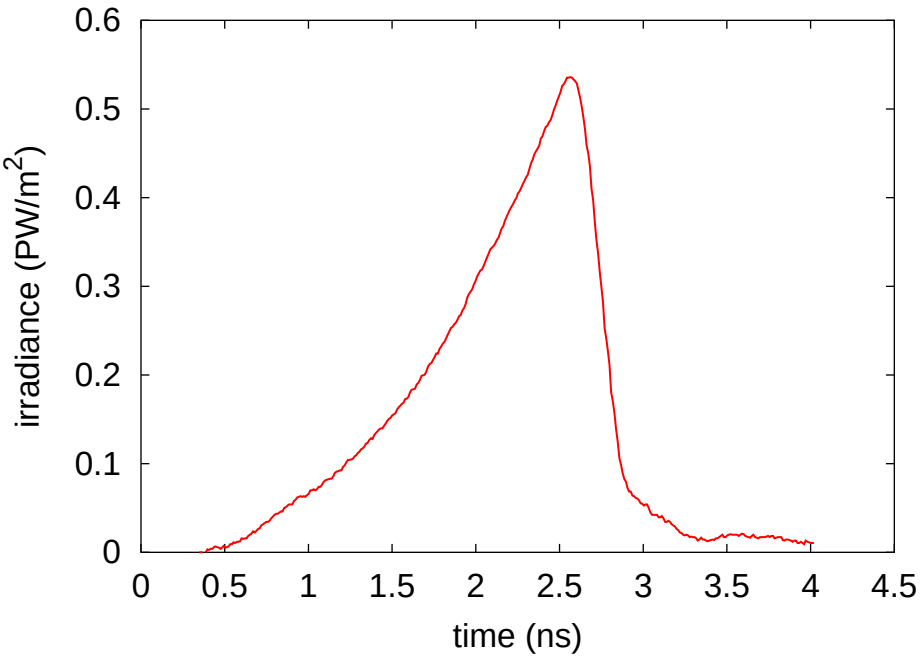

Figure 15: Laser irradiance history from shot 15022.

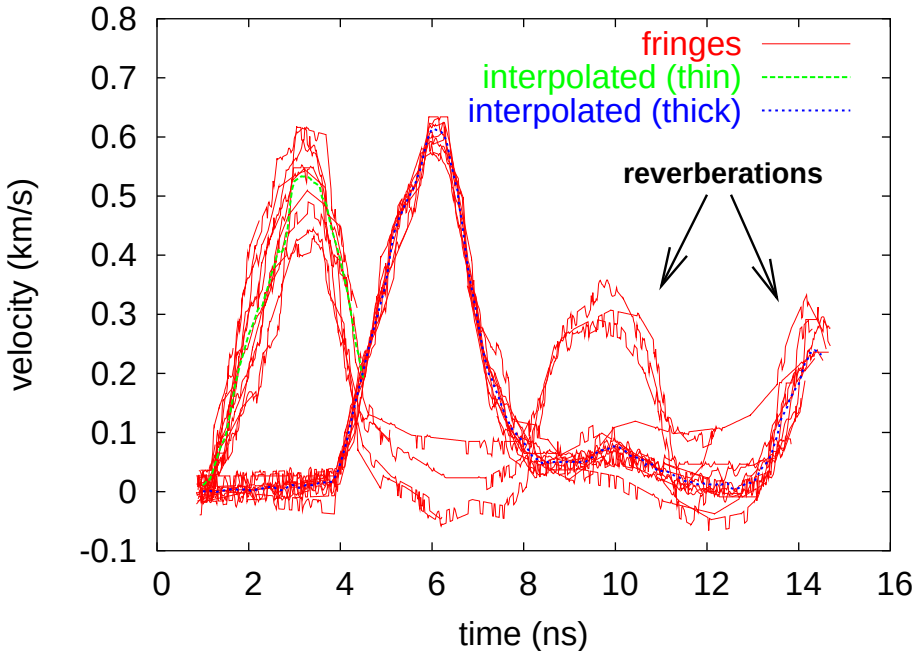

Figure 16: Velocity histories from shot 15022 (30 and 59 μm Si; 13 J).

4 Analysis

For the experiments where the surface velocity was measured for samples of two different thickness, we used an approximate analysis to deduce loci of isentropic compression from each experiment [5]. The surface velocity history from each sample $u_s(t)$ is used to estimate the velocity inside the material $u(t)$, assuming that the presence of the surface does not complicate the relationship between the different velocity histories. For a free surface velocity, $u(t) \simeq u_s(t)/2$. This relationship – and the assumption that the velocities are not complicated by waves reflected from the surface – is reasonable at the relatively low velocities obtained in these initial experiments.

Considering the time at which the velocity from each sample reaches a given value, the Lagrangian wave speed can be estimated as a function of velocity,

$$c_L(u) = \frac{\Delta x}{\Delta t(u)}, \tag{1}$$

where Δx is the difference in thickness between the two samples and $\Delta t(u)$ is the difference in time at which each record reaches a speed u. The normal stress and density can then be inferred along the isentrope by integrating

$$\frac{d\sigma}{du} = \rho_0 c_L \tag{2}$$

$$\frac{d\sigma}{d\rho} = c_E^2, \tag{3}$$

$$\tag{4}$$

where c_E is the Eulerian wave speed and

$$c_L = \frac{\rho}{\rho_0} c_E \tag{5}$$

[5].

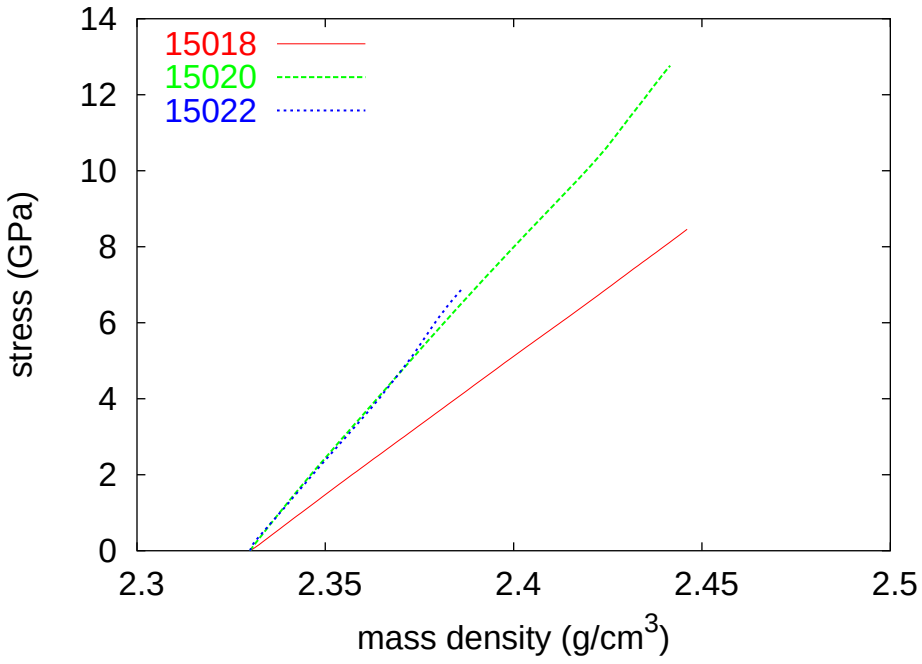

Figure 17: Comparison of isentropes deduced from experiments on pairs of (100) silicon crystals.

We analyzed the silicon data from shots 15018, 15020, and 15022 in this way, using the single interpolated velocity history from each sample. The stress – density relations from the shots with the highest and lowest energy (15020 and 15022) agreed well, though the relation from the other shot (15018) was significantly different. The difference was nominally within the uncertainty inferred from the scatter in velocity histories, suggesting that the interpolation may not have been performed consistently for all shots, though the inconsistency was not found. (Fig. 17.)

The isentropes were compared with previous predictions of the isostatic equation of state of silicon, calculated using *ab initio* quantum mechanics [6]. In the range of compressions explored by the LICE experiments, the shock Hugoniot and isentrope predicted theoretically were not significantly different. Gas gun experiments performed on large samples of silicon and reduced using standard shock wave techniques [7] lay close to the *ab initio* Hugoniot. The LICE isentropes were significantly stiffer, as one would expect when comparing isostatically and uniaxially compressed states since in uniaxial compression the normal stress includes a contribution from elastic shear. (Fig. 18.)

Ab initio techniques are also suitable for predicting states produced in uniaxial compression, and elastic stress – strain relations have previously been calculated for silicon [8, 9]. Quantum mechanical calculations of this type fail to reproduce the observed mass density at STP, and the correction developed for the equation of state cannot be applied directly to stress – strain calculations; this is an area of current research. For this reason, we investigated the sensitivity to variations in mass density by comparing the LICE data with quantum mechanical calculations using different values of the basal lattice parameter. The quantum mechanical calculations were adjusted by adding a constant offset to each in order to make the pressure – density relation pass through the observed STP state. The calculations agreed quite well with the isentrope deduced from shot 15018, i.e. the least stiff isentrope. The LICE relation was still slightly stiffer than the calculations; this is not implausible as, unlike the experiments, the calculations were isothermal. (Fig. 19.)

No attempt was made to analyze or simulate these experiments using more accurate techniques [10]. Our preferred starting point would be a series of forward simulations using continuum mechanics, but this would require a reasonable strength model for silicon. Simulations of this type are planned for the future.

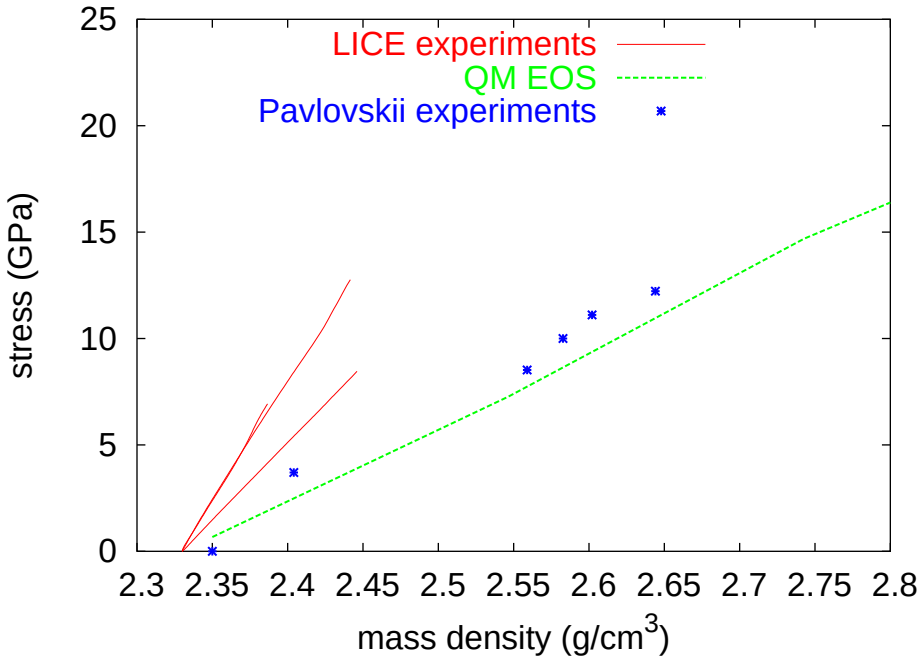

Figure 18: Comparison of isentropes with principal Hugoniot from theoretical isostatic equation of state and shock wave measurements on silicon.

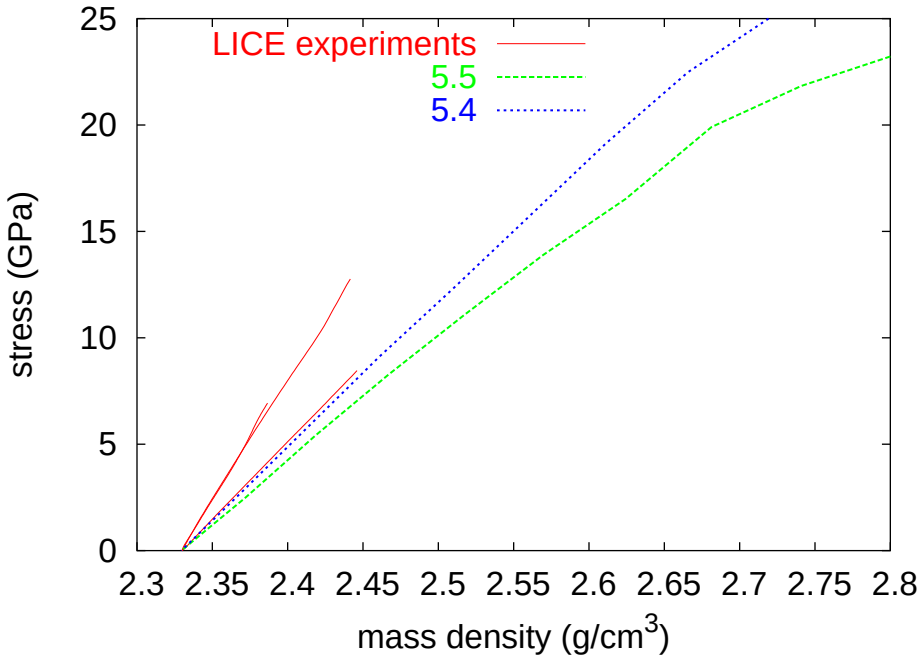

Figure 19: Comparison of isentropes with predicted stress during uniaxial deformation in silicon, for different values of the basal lattice parameter (in Å).

5 Discussion

Isentropic compression waves were readily induced by shaping the temporal history of a laser pulse and irradiating the sample directly. When using silicon samples with an aluminum coating on the opposite surface from the drive beam, the fringe quality was poorer and the fringes disappeared around the time of the peak free surface velocity. The most likely cause is debonding of the aluminum, so we recommend against aluminizing the surface in future experiments.

In some of the experiments, the streak camera record of the fringes captured a reverberation following the initial compression and release. The peak velocity associated with the reverberation did not exceed 250 m/s, irrespective of the peak velocity from the first wave. This suggests the presence of a limiting mechanism such as plastic flow. We plan to investigate the reverberation in future studies, as it requires a continuum mechanics model for silicon which is more complete than any currently available.

In the silicon experiments, except where obscured by debonding aluminum, the surface velocity decreased by up to 0.6 ± 0.1 km/s following the initial peak, returning to zero if the initial peak was low enough. Using an approximate relation for spall strength [11],

$$\sigma = \frac{1}{2}\rho_0 c_0 \Delta u, \tag{6}$$

where ρ_0 and c_0 are the mass density and sound speed at STP and Δu is the reduction in velocity following the peak, the spall strength for (100) silicon on the time scales probed by these experiments was estimated to be 4.8 ± 0.8 GPa.

Most of the streak camera records appeared to exhibit structure on the rising or falling part of the velocity history. Some of this was probably caused by speckle in the fringe pattern, though it is possible that some was caused by the onset of plasticity or phase transition. The detailed interpretation will be addressed through future continuum mechanical simulations.

6 Conclusions

The pulse-shaping capabilities of the TRIDENT laser were used to generate isentropic loading in samples irradiated directly with 527 nm light. Surface velocimetry indicated that smooth compression waves were produced. Ramping the irradiance up to $\sim 2\,\mathrm{PW/m^2}$ over a 2.5 ns pulse, pressures of up to about 10 GPa were generated in samples of silicon and aluminum. The compression waves did not steepen into shocks over a sample thickness of several tens of micrometers. The energy in the drive pulse was well below the maximum available from TRIDENT, so it seems quite possible to use this technique to produce isentropic compression up to several tens of gigapascals in materials of higher atomic number and of a similar thickness.

Experiments were performed on pairs of silicon samples of different thickness. Isentropes were deduced from the resulting data, using an approximate technique which should be reasonably accurate over the pressures attained. The isentropes were significantly stiffer than the isostatic equation of state, but showed better agreement with theoretical predictions of the response of silicon crystals to uniaxial compression.

Acknowledgments

We would like to thank the TRIDENT staff including Tom Hurry, Tom Ortiz, Fred Archuleta, Nathan Okamoto, and Ray Gonzales for their hard work on the experiments. Ron Perea (MST-7) provided the silicon samples, and José Velarde made the re-usable target holder. George Kyrala reviewed this report and suggested valuable improvements. We are particularly grateful to Cris Barnes, whose encouragement led directly to the work described here.

References

[1] J.R. Asay, in *Shock Compression of Condensed Matter – 1999*, edited by M.D. Furnish, L.C. Chhabildas, and R.S. Hixson (American Institute of Physics, New York, 2000), p. 261.

[2] D.C. Swift, *TRIDENT materials shots (Flying Pig 2), August 2002*, Los Alamos National Laboratory memo P-24-U:2002-222 (2002).

[3] R.P. Johnson (Los Alamos National Laboratory), design of VISAR system for widely variable delays, unpublished (2001).

[4] D.C. Swift, *Analysis of TXD and VISAR experiments on shock waves in beryllium crystals*, Los Alamos National Laboratory report LA-UR-01-3410 (2001).

[5] D.B. Reisman, A. Toor, R.C. Cauble, C.A. Hall, J.R. Asay, M.D. Knudson, and M.D. Furnish, *Magnetically driven isentropic compression experiments on the Z accelerator*, J. Appl. Phys. **89**, 1625 (2001).

[6] D.C. Swift, G.J. Ackland, A. Hauer, and G.A. Kyrala, *First principles equations of state for simulations of shock waves in silicon*, Phys. Rev. B **64**, 214107 (2001).

[7] M. N. Pavlovskii, *Formation of metallic modifications of germanium and silicon under shock loading*, Sov. Phys. - Solid State **9** 11 (1968).

[8] D.C. Swift, in *Shock Compression of Condensed Matter – 1999*, edited by M.D. Furnish, L.C. Chhabildas, and R.S. Hixson (American Institute of Physics, New York, 2000), p. 125.

[9] D.C. Swift and G.J. Ackland, *Quantum mechanical predictions of non-scalar equations of state and non-monotonic elastic stress-strain relations*, submitted to Phys. Rev. Lett. (2002).

[10] D.B. Hayes, *Backward integration of the equations of motion to correct for free surface perturbations*, Sandia National Laboratories report SAND2001-1440 (2001).

[11] A.V. Bushman, G.I. Kanel', A.L. Ni, and V.E. Fortov, *Intense Dynamic Loading of Condensed Matter*, (Taylor and Francis, Washington DC, 1993).